FISHEYE PHOTOGRAMMETRY: TESTS AND METHODOLOGIES FOR THE SURVEY OF NARROW SPACES

Luca Perfetti [1,*], Carlo Polari [1], Francesco Fassi [1]

[1] 3DSurvey Group, Politecnico di Milano, Architecture, Built environment and Construction engineering (ABC) Department

Commission II

KEY WORDS: Fisheye, Photogrammetry, Survey, Cultural heritage, Narrow spaces, lenses, Projection

ABSTRACT:

The research illustrated in this article aimed at identifying a good standard methodology to survey very narrow spaces during 3D investigation of Cultural Heritage. It is an important topic in today's era of BIM modelling applied to Cultural Heritage. Spaces like staircases, corridors and passages are very common in the architectural or archaeological fields, and obtaining a 3D-oriented survey of those areas can be a very complex task when completeness of the model and high precision are requested. Photogrammetry appears to be the most promising solution in terms of versatility and manoeuvrability also considering the quality of the required data. Fisheye lenses were studied and tested in depth because of their significant advantage in the field of view if compared with rectilinear lenses. This advantage alone can be crucial to reduce the total amount of photos and, as a consequence, to obtain manageable data, to simplify the survey phase and to significantly reduce the elaboration time. In order to overcome the main issue that arise when using fisheye lenses, which is the lack of rules that can be employed to design the survey, a general mathematical formulation to precisely estimate the GSD (Ground Sampling Distance) for every optical projection is presented here.
A complete survey of a real complex case study was performed in order to test and stress the proposed methodology, and to handle a fisheye-based survey from beginning to end: the photogrammetric survey of the Minguzzi Staircase. It is a complex service spiral-staircase located in the Duomo di Milano with a total height of 25 meters and characterized by a narrow walkable space about 70 centimetres wide.

1. INTRODUCTION

1.1 Fisheye lenses to survey narrow spaces

Nowadays the use of BIM technologies and 3D representations in the architectural field increased the demand of 3D survey techniques. For this reason, in the last few years, the world of Cultural Heritage has seen a strong and constant development of survey technology and practises aiming at acquiring complete, "dense", and high-precision 3D information. Architectural monuments, in particular, were studied in their shapes and textures focusing mainly on representative spaces. This happened because the process was usually carried out for restoration and conservation purposes, thus centring the attention of the superficial, noble parts of the "object", the "skin of the building". The classical 2D drawings or orthophotos have been so far sufficient to represent the objects. In this context, less attention was obviously paid on "service spaces" which are less important from an artistic point of view and therefore largely excluded from any kind of dedicated and complete representation. However, when dealing with a full 3D appraisal of complex architectures, these secondary spaces (such as staircase, corridors and passages) play an important role; if the goal of the survey is to produce a 3D BIM model of the building, they cannot be forgotten only because of their reduced accessibility.
Moreover, the survey technology for terrestrial applications nowadays consists in range- or image-based instrumentations that work well in large and illuminated areas like naves, cloisters or rooms. They normally provide accuracy and resolution down to millimetres or centimetres (1:50-1:100 representation scale) with a normal functional range between 1 and 100 meters distance. No close range methodologies are appropriate for surveying "service rooms" normally characterized by very narrow spaces, reduced illumination and irregular complex geometry. Due to the lack of the "right instrument", surveying those areas results oddly the most time-consuming and difficult part of the measurement campaign.
This paper would like to answers the increasing demand of an alternative survey technique that can be reliable and efficient in the difficult task of surveying narrow spaces and that can either replace or be used together with the consolidated technology involved in typical investigation activities (i.e. laser scanners). The aim is to identify a process and a methodology that can be efficient if applied to the case studies of complex interior architectural environments.
The close range photogrammetry technique is chosen in order to achieve this goal trying to push one step further the understanding of fisheye lenses, both in theory and in practice.
Fisheye photogrammetry turned out to be the most promising solution (Marčiš, 2016) (Covas, 2015) in comparison with other consolidated tools, such as traditional laser scanners or new developed hand-held mobile mapping devices, such as Kinect style mobile devices or Slam 3D scanners. Spaces like corridors, tunnels or staircases represent challenging tasks for each of these techniques. Traditional range-based instruments struggle against the lack of operating space, while the hand-held solutions, according to the first tests, fail to match the precision and resolution required for Cultural Heritage architectural survey showing reliability and repeatability problems. Trying to solve the main issue of surveying narrow areas using photogrammetric approach, the choice between traditional lenses (i.e. rectilinear lenses) and fisheye lenses is almost compulsory, in order to avoid the enormous number of shots required to cover the entire surface

* Corresponding author

with a "generous overlap" between pictures. The advantage of a wider field of view (FOV) alone can be crucial to obtain manageable data, where rectilinear lenses approach would be prohibitive. This advantage comes with a price: the issues with the use of fisheye optics are numerous and linked to the fact that fisheyes are not just wider rectilinear lenses. The different type of optical projection hampers the operator ability in designing the survey and, as consequence, his control over the result. The risk to fail the measurement and to lead to a warped model (bended, stretched, compressed…) as a result of a wrong photogrammetric planning is very high. (Nocerino, 2014)
This article's goal is to approach the problem mainly focussing on the designing phase of the survey, when the operator has to take into account the concept of GSD (Ground Sampling Distance), the overlap between pictures and the organisation of the capturing scheme. This phase became very complex once the fisheye approach is chosen.

1.2 Difference between fisheye lenses and rectilinear lenses

The main issue using fisheye lenses concerns the high probability to get incomplete, poor and inconsistent results. The main drawback appears to be the difficulty to take control of the variables that could invalidate the photogrammetry process. This happens when one tries to use the same consolidated pipeline designed for the rectilinear projection lenses with fisheyes. Considering them just being wider FOV lenses could cause failure in the photogrammetric. A fisheye lens is not a rectilinear lens: it is critical to understand the difference between the different optical projections.
A very wide FOV and a very short focal lens do not make a lens a fisheye. It is the particular interaction between the two, focal length and field of view, which make the difference. The relation between the two parameters, which consist in the optical function, define the characteristic of the lens. Each optical function holds its own relation between focal length and field of view. To the same focal length, a different FOV can corresponds for each available optical projection. The main advantage of fisheye lenses is that the incoming light beam converge on a circumference of shorter radius on the sensor than a rectilinear lens at a given focal length.
The main type of available optical projections are the followings (Ray, 2002) (Kannala, 2006):

Rectilinear:	$r = f\,\tan(\theta)$	(1)
Equidistant:	$r = f\,\theta$	(2)
Equisolid:	$r = 2f\,\sin\left(\frac{\theta}{2}\right)$	(3)
Stereographic:	$r = 2f\,\tan\left(\frac{\theta}{2}\right)$	(4)
Orthographic:	$r = f\,\sin(\theta)$	(5)

Where r = distance from the centre of the sensor
f = focal length
θ = angle of incidence of the light beams

The first one is the classical "pin-hole" projection (Figure 1) also known as perspective projection (when the medium in which the light beams travel remains the same both outside and inside of the dark camera). The others are all different type of fisheye projections.
It must be noticed that a FOV of 180° is impossible with the perspective projection; with the fisheye projections, instead, a 180° FOV angle is always possible. The equidistant and equisolid angle projections can theoretically reach 360° (depending both on the focal length and the sensor size). The widest fisheye lens ever designed, though never pushed to mass production, is an equidistant based projection which can reach 270° field of view: the Nikon 5.4mm f/5.6 (U.S. Patent 3,524,697).

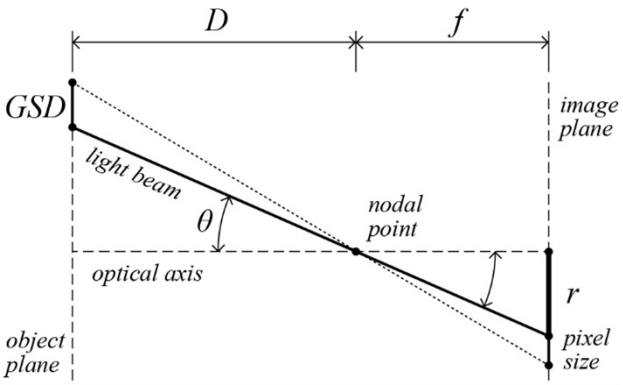

Figure 1. Pin-hole projection scheme. In this scheme it is easy to recognize a similarity between triangles. The following ratio $f : D = pixel\ size : GSD$ is a very simple and standard tool that gives to the survey operator control above the results of the survey itself. The concept of GSD and the possibility of calculate/impose it, gives the link to the precision of the two or three-dimensional representation to be extracted from the survey.

2. GENERAL MODEL TO CALCULATE THE GSD FOR FISHEYE LENSES

2.1 The distortion of fisheye lenses: not uniform GSD through the frame

Every single optical projection distorts reality; however, one has to make a distinction between the distortion of the mapping function itself and the distortion between that theoretical model and the physical lens.
The first one is a characteristic of the projection model and of how it maps the three-dimensional world on a two-dimensional surface. This type of distortion exists both in the ideal and in the real lens and can be measured a priori.
The second type of distortion is usually a tiny variation in the behaviour of the lens from the reference mapping function. This distortion can be attributed to a number of imperfections in the manufacture process of the lens, starting from the design, passing through the construction down to the assemblage. In the photogrammetry pipeline, normally the two components are calculated at the same time during the calibration phase, and the first part of the distortion is considered in the designing phase of the survey by using the simple scheme in Figure 1; this scheme takes into account the way in which the rectilinear mapping function projects the 3D world into a 2D surface.
Also in the case of fisheye lenses, both components of the distortion have to be considered in software computation by the calibration model; even more important: during the designing of the acquisition phase it is crucial to consider the first component of the distortion, the characteristic of the mapping function itself. The mapping function of a lens strongly influences the outcome pictures, their resolution and consequently the GSD, which is not uniformly distributed on the frame using fisheyes.
Even if not in the same way, all fisheye lenses, if compared with a rectilinear lens, compress a larger field of view in a shorter radius from the centre of the sensor at the same focal length. This fact entails a strong decrease in resolution: while the resolution

decreases, the GSD increases in size. Moreover, the GSD degradation in fisheye optics is not constant across the sensor and varies following a non-linear function, which depends on the mapping function. As results, the GSD gets worse with increasing FOV until the point where the field of view reaches 180° in which the GSD is equal to infinity. (Pierrot-Deseilligny, 2011)
This has important consequences on the required overlap among neighbouring images and consequently on the base distance/capturing distance ratio to be respected during acquisition. Moreover, it can influence the matching process by preventing the correct alignment among the images and reducing the resolution and the quality of the generated DSM. At this stage (acquisition design), it is not necessary to have an accurate estimation of GSD distortion inside image but knowing it in an approximate way is essential to setup the correct captureing geometry and to pre-elaborate the images in order to use only images with enough resolution according to the final representation scale.
The consolidated methodology used when designing the photogrammetric survey is strongly based on the pin-hole projection scheme (Figure 1) but, here, this scheme fails and cannot be used.

2.2 Mathematical GSD calculation

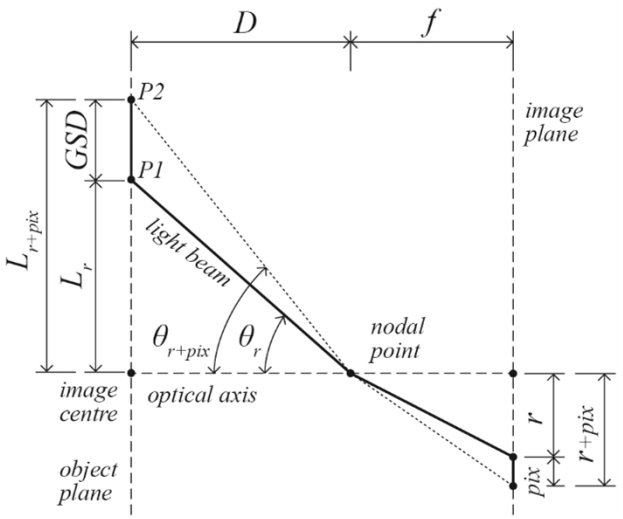

Figure 2. Illustration of the relation between pixel size and GSD for each projection function.

When designing the survey with fisheye lenses, we have to measure the GSD, doing that using a mathematical theoretical model allows to evaluate different lenses with different mapping function a priori. A GSD formula has to be calculated for each optical projection and these formulas can be extracted from the generic mathematical model presented.
The new model, unlike for the pin-hole scheme, has to take into account the distance from the centre of the sensor and, most important, the optical projection peculiarity. GSD varies depending on the position on the frame, therefore it we should include the parameter **r**, that represents the radius distance from the centre of the frame on which a light beam of angle theta is projected depending both on the mapping function and on the focal length.
By reversing the optical projection function of a fisheye lens, it is possible to calculate the angle theta of the incoming light beam for each **r**, the incoming light beam of angle $\boldsymbol{\theta_r}$ intersects the object plane on the point **P1** distant $\mathbf{L_r}$ from the image centre. At the same way, the incoming light beam of angle $\boldsymbol{\theta_{r+pix}}$ which hits the sensor at a distance of **r+pix**, intersects the object plane on the point **P2** distant $\mathbf{L_{r+pix}}$ from the image centre.
To write the theoretical formulation of GSD depending also on **r** we can first write the following (8).

$$GSD = L_{r+pix} - L_r \tag{6}$$

Knowing $\mathbf{L_r}$ and $\mathbf{L_{r+pix}}$ from right angled triangles theorems (7, 8), we can write the general GSD formula (9) coming from (6).

$$L_r = D \cdot \tan(\theta_r) \tag{7}$$

$$L_{r+pix} = D \cdot \tan(\theta_{r+pix}) \tag{8}$$

$$GSD = D \cdot \tan(\theta_{r+pix}) - D \cdot \tan(\theta_r) \tag{9}$$

Here, $\boldsymbol{\theta_r}$ and $\boldsymbol{\theta_{r+pix}}$ finally depends on the optical projection of the lens, where theta is always related to **r**. It is possible to reverse the mapping function of the chosen lens in order to explicit theta. We choose the stereographic optical function (4) to obtain the following (10).

$$\theta = 2\arctan\left(\frac{r}{2f}\right) \tag{10}$$

obataining (11) in this way:

$$L_r = D \cdot \tan\left[2\arctan\left(\frac{r}{2f}\right)\right] \tag{11}$$

It is possible to do the same with $\mathbf{L_{r+pix}}$, and finally to write the GSD equation for the stereographic fisheye projection (12) by substituting $\mathbf{L_r}$ and $\mathbf{L_{r+pix}}$ in the first formulation of GSD (6).

$$GSD = D \cdot \left\{\tan\left[2\arctan\left(\frac{r+pix}{2f}\right)\right] - \tan\left[2\arctan\left(\frac{r}{2f}\right)\right]\right\} \tag{12}$$

The equation above (14) allows to express the GSD considering both the classical parameters normaly involved in photogrammetry, D, f and pixel size with the addition of **r** to take into acont the GSD degradation through the frame.
The rightness of the mathematical model is confirmed also for the rectilinear projection where after simple calculation it is possible to demonstrate that the GSD is indipendent from the parameter **r**.
It is also possible to apply it to other types of optical projections: equidistant and equisolid. It has been decided not to focus on the orthographic projection because it is considered a priori as the worst case, not suitable for photogrammetric purposes. The formulas for calculating the GSD with equisolid (13) and equidistant (14) projections are herein shown:

$$GSD = D \cdot \left\{\tan\left[2\,\mathrm{arcsen}\left(\frac{r+pix}{2f}\right)\right] - \tan\left[2\,\mathrm{arcsen}\left(\frac{r}{2f}\right)\right]\right\} \tag{13}$$

$$GSD = D \cdot \left[\tan\left(\frac{r+pix}{f}\right) - \tan\left(\frac{r}{f}\right)\right] \tag{14}$$

Being able to calculate the GSD values for the different optical projections, it is possible to compare them toghether in the same graph, showing the decrease of the GSD from the center to the edge of the image.
The comparison should be performed chosing some fix parameters: focal length f, pixel size and capturing distance D.

Pixel size (PX)	Focal length (f)	Taking distance (D)
0,00489 mm	12 mm	2,5 m

The presented system allows the operator to calculate the resolution distribution across the images beforehand, and, as a consequence, to monitor the minimum value of GSD for the various optical projections; since the lower resolution will influence on the outcome of the photogrammetric process, it is important to understand which parts of the images can be used in relation to the chosen representation scale. This makes it possible to calculate the radius **r** of the maximum circumference within which the resolution is compatible with the chosen scale: the remaining part, expressing a resolution lower than the acceptable minimum, can be discarded (Figure 3, Figura 4).
In the scale 1:50, for instance, typically used in the survey of cultural heritage, the minimum resolution that the photographs must have is expressed by the value of the GSD, maximum 10mm. At this point, according to the optical projection in use, it is possible to calculate the value of the radius **r** which defines the circumference that places the photographic area with sufficient resolution on the inside, and the one with insufficient resolution on the outside. This information can be used to crop the images, discarding the marginal areas to keep only the portion on the inside of the aforementioned circumference.

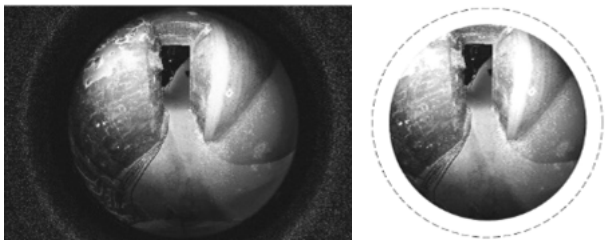

Figure 3. Original picture taken using a fisheye lens and the same image cropped to comply the desired scale.

In this case (Figure 4), considering a distance D of 2.5 meters and a focal length f of 12mm, if one wants to use a fisheye lens with equisolid projection, one would have to discard the whole image area beyond the 12mm radius from the center of the sensor.
If one wants to use a fisheye lens with equidistant optical projection, the radius should correspond to about 13mm, should correspond to 16mm using a stereographic fisheye lens. It is interesting to note how the rectilinear projection is characterized by a constant GSD value for any **r**.
The graph in Figure 5 shows the different angles of FOV that each optical projection is able to achieve in relation to the radius **r**. It is therefore understood that for an ultra wide-angle rectilinear lens with 12mm focal length, the maximum FOV angle that can be reached on the image diagonal is 120°.
The same value can be obtained with a fisheye equisolid projection at the distance **r** of 12mm from the center of the sensor. This distance corresponding to the maximum value of **r** that provides an appropriate resolution for the 1:50 scale; therefore, in terms of FOV, there is no advantage in using equisolid fisheye lenses rather than rectilinear ones under these conditions and for the same representative scale. However, with the equidistant projection the maximum FOV that can be reached is 130° and with the stereographic projection lens, a FOV angle of 140° can be reached instead.

By drawing a parallel between the two charts, the operator can predict in advance the behavior of fisheye lenses as well as rectilinear lenses, managing to check, always in advance, if there is a significant advantage to using one over the other.

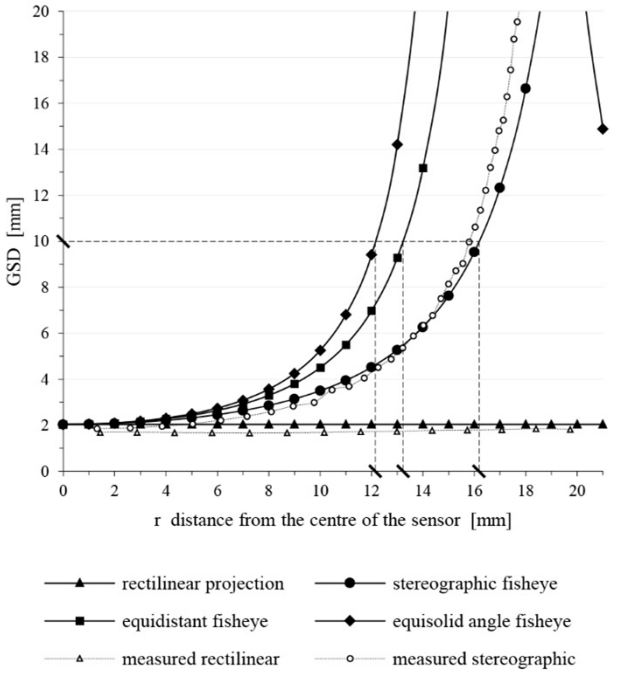

Figure 4. Comparision graph among different optical projection behaviour. The simulation is done for a camera with a pixel size of circa 4,9 Microns, a focal length of 12mm and a taking distance from the object of 2,5 m.

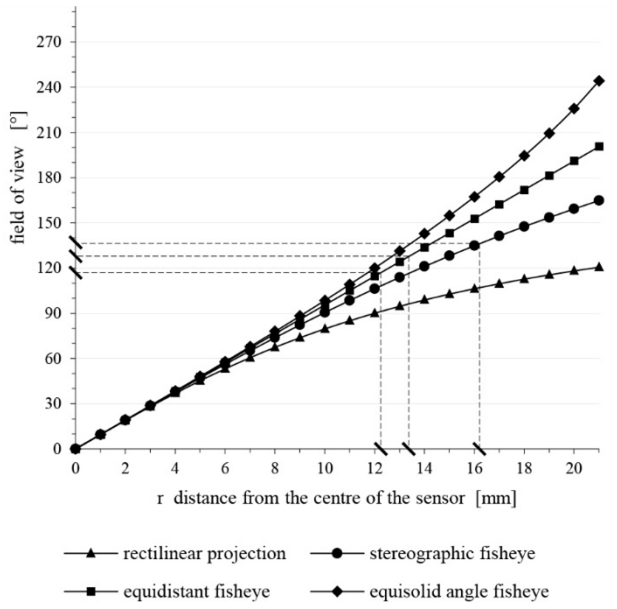

Figure 5. Field of view that can be reached with different optical projection. The simulation is done using the same parameters described in Figure 4.

3. EXPERIMENTAL AND VALIDATING TESTS

3.1 Experimental test on GSD distribution

The graph in (Figure 4) reveals the behavior of the different optical projections that has to be taken into consideration in order to correctly design the survey and obtain the desired results. However, the actual distortion of any physical lens is

characterised by some small differences when compared to their theoretical mathematical model.
Therefore, in order to verify the theoretical model, a test was conducted, making it possible to measure the decrease in the GSD with two fisheye lenses: Samyang 12 mm fisheye stereographic and Sigma 8mm fisheye equisolid.
The aim of this test was to obtain a sort of "scale factor" able to parameterize the fisheye lens behavior, in terms of lens distortion and in relation with the rectilinear theoretical parameters. This will then take two aspects of the distortion into consideration at the same time: the difference between the two optical projections in question (rectilinear and fisheye), as well as manufacturing defects of the lens.
In order to obtain this "scale factor" a target was designed with a metric scale of about 2.5m length and a minimum unit of 5 cm length. The target was attached horizontally on a wall to be photographed at a distance of 50 cm, while the camera, on the other way, was positioned in a tilted position. In such a way, in the frame, the target was lying exactly on the diagonal of the sensor with the metric scale, on which the measurements are based, passing exactly into the center of the frame. At this stage, a great deal of attention was paid to ensure the maximum parallelism and centering of the sensor with the target.
Bearing in mind that the (theoretical) rectilinear projection produces, on the sensor, equal intervals from the photographed metric target regardless of the position in the frame; it is therefore possible to calculate the length of these intervals projected on the sensor, if the capturing distance and the focal length are known beforehand.

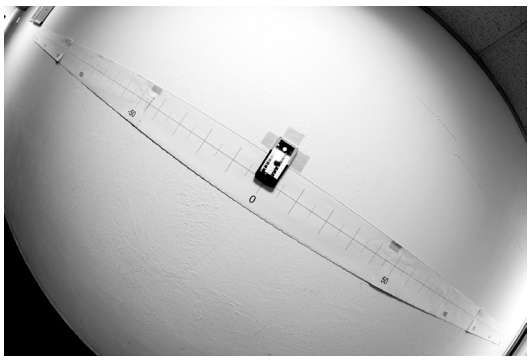

Figure 6. Photo of the metric target obtained with a diagonal fisheye, the Samyang 12mm.

The picture of the target obtained with the fisheye lenses deviates greatly from this behavior, reproducing very different intervals along the diagonal of the image (Figure 6). The intervals of the target were measured on the real obtained photograph by scaling it on the sensor size. Finally, by performing the ratio between the actual intervals (measured from the real fisheye picture) and the theoretical intervals (rectilinear projection), it is possible to obtain a percentage factor that encloses the effect of the two components of the distortion. By calculating this percentage factor at different points on the diagonal of the image, it is possible to obtain a map of proportionality for each of the tested fisheye lenses. Finally, with this map of proportionality it is possible to calculate the GSD considering a rectilinear lens and then "scale" the outcome to obtain the GSD expressed for the fisheye one. Although the behavior of the real lens (fisheye) differs slightly from the theoretical one (Figure 4), the variation is sufficiently limited to allow the theoretical model to be used for the design of survey with real optics.

3.2 Experimental tests on ideal capture geometry: base distance/capturing distance ratio

The next step it is to define an optimal capturing geometry on which the photogrammetric survey can be based. Although the capturing geometry varies from case to case depending on the volumetric features of the survey object, it is important to define the base distance/capturing distance ratio which underlies the capturing geometry design.
While with rectilinear projection lenses the calculation of the base distance/capturing distance ratio comes from the percentage of overlap between neighbouring picture (about 70-80%), with fisheye lenses this approach fails. Due to the very wide field of view angle of fisheye lenses, the overlap of two neighbouring pictures lying on the same plane would be huge, would even equal to infinity when the FOV is equal to 180° or more. It is clear that the percentage of overlap it is not a useful parameter on which to base the capturing geometry. Many empirical tests were held in order to overcome that issue: a photogrammetric survey of a straight wall was performed using a high number of photographs precisely spaces out; little by little some pictures were removed to the point to obtain a correct survey with a minimum number images.
After these tests, a 1:1 base distance/capturing distance ratio turned out to be the best ratio to be used with fisheye lenses. This information makes possible to design a suitable capturing geometry when the working distance is known.

Figure 7. Capturing phase of the straight wall test.

4. REAL COMPLEX CASE STUDY

4.1 The Minguzzi staircase

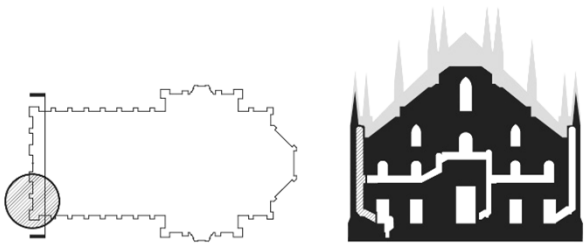

Figure 8. Location of the Minguzzi spiral staircase in the Milan cathedral.

In order to verify the effective usability of fisheye photogrammetry technique for the survey of narrow spaces, and the correctness of the described methodology, the technique was applied to the survey of a complex architectural environment, the Minguzzi staircase of Milan Cathedral. The test is part of a more extensive research project that includes the survey of the entire monumental complex of the Duomo di Milano and the creation

of a complete 3D model of the cathedral to be structured and used in a BIM system prototype. (Fassi, 2015)
The Minguzzi staircase is a marble stone spiral staircase located inside the right pylon of the main facade of the cathedral. Along its extension of about 25m in height, it connects three different levels of the building: at the upper end the lower level of the roofs; in the middle the central balcony of the facade; and at the base the floor of the church.

Figure 9. Internal view of the Minguzzi staircase during the photogrammetric survey.

The staircase is extremely dark. The artificial illumination is of poor quality, and there are only a few openings towards the outside placed at regular intervals. From the inside, these openings are relatively large (85cm) and deep (circa 2m) due the considerable thickness of the wall: they narrow down noticeably towards the outside and end up as small vertical embrasures (30cm width). At the center of the staircase, there is a stone column with a diameter of about 40cm around which the ramp rolls up; the space left for the passage is extremely narrow, about 70cm. This extremely narrow space was complex enough to represent a serious test of our research topic. In this situation, there is simply no space to use a normal terrestrial scanner instrumentation. Moreover, many other factors would nullify the whole scan, making the job unnecessarily time-consuming and burdensome in terms of amount of data: the minimal operational range of the instrumentation and the shadow areas due to tripod legs combined with the spiraling geometry of the stairs itself could be the main issues. Mobile scanners or hand-handled instrumentation cannot be used in this case because of the impossibility to create loops during the acquisition, which is an indispensable prerequisite to use this type of technologies.
For all these reasons, the case of study provides an ideal environment to put the fisheye photogrammetric system to the test.

4.2 The survey phase

Before moving on to the field, it was imperative to fully understand the geometry of the object in order to properly design the capturing geometry, and to completely cover all the spaces useful for the re-design of the staircase. The adopted shooting geometry was created by dividing the image acquisitions phase into five main placements of the camera. In addition, a series of integration acquisitions were taken to complete some complex areas.

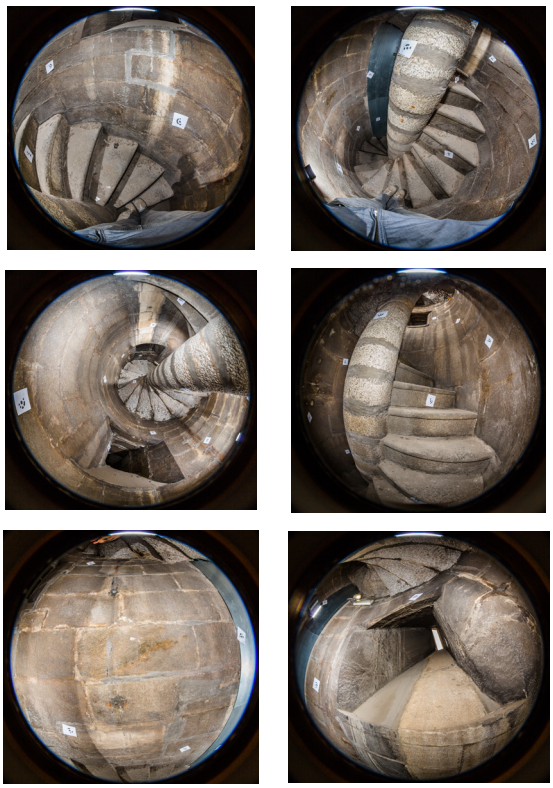

Figure 10. Five pictures which compose the capturing geometry, plus one detail picture (bottom right) of one opening.

The shooting geometry in question has been designed by taking into account a good amount of overlapping among images, as empirically deduced from above tests (Chapter 3.2) a 1:1 base distance/capturing distance ratio was used.
The survey was carried out with two different cameras and three different lenses: Canon 5D mark III coupled with Sigma 8mm circular fisheye and Nikon D810 coupled with Samyang 12mm diagonal fisheye and Sigma 12-24mm rectilinear lens. The whole image acquisition process was accomplished with the aid of three portable synchronized photographic flashes, which made possible to light up the otherwise too dark area of the staircase. 220 photogrammetric encoded markers were distributed homogeneously on the main surfaces in order to i) optimize the alignment as well as scaling and georeferencing the point cloud of the object, ii) checking the accuracy of the photogrammetric bundle adjustment, and last but not least iii) comparing the results among the different lenses.
The different field of view and the GSD calculated value have determined the number of shots needed, as shown in the table below.

	8mm fisheye	12mm fisheye	12mm rect.
N° photos	764	889	945

The idea was to survey the stairs several times using different lenses in order to compare the results and verify the accuracy in relation to the use of different optical projection.
Some scans using TLS Leica C10 where performed at the base and at the top of the stair. This scans were georeferenced in the topographic network built for the cathedral survey activity; some photogrammetric targets were measured at this stage as well. These measurements were performed in order to check the accuracy of the survey and in particular if any bending, stretching or compression distortion occurred to the final model. In this way, we had two check-stations at the base and at the top of the stair. In the interior of the staircase, where no additional instrumental check was possible, many reference distances among markers were taken in order to manually monitor the alignment.

4.3 The data elaboration

First of all, before proceeding with the software elaboration, it was important to apply the discussed methodology to crop the marginal areas of the pictures when not suitable for the desired scale. For these tests the chosen representation scale was 1:50; according to that, all the images taken with fisheye lenses were cropped when the GSD where higher that the 10mm maximum: for the Canon 5D coupled with 8mm equisolid fisheye, the cutting radius is 8,20mm from on the sensor; for the Nikon coupled with 12mm stereographic fisheye, the radius is 18,5mm. no cropping is needed for the rectilinear lens.

Photogrammetric process

	Canon 5D 8mm fish.	Nikon D810 12mm fish.	Nikon D810 12mm rect.
Alignment	0,032 m	/	0,055 m
Marker optimization	0,031 m	0,013 m	0,051 m
Scale bar optimization	0,010 m	0,014 m	0,051 m
Optimization over topography	0,009 m	0,014 m	0,051 m

Figure 11. Residual errors for the different elaboration during the photogrammetric process.

Agisoft Photoscan was used in the elaboration phase, one of the most powerful software to process big amount of images. Some tests were also carried out using MICMAC: good results were obtained when using few photos, but it was impossible to complete the entire project just because of the high number of involved images.
For all the three tests (Canon 5D Mark III with 8 mm fisheye, Nikon D810 with 12 mm fisheye and 12-24 mm rectilinear), but in particular for those with the fisheye lenses, it was necessary to manually intervene on the alignment after the automatic process, to provide additional manual constraints and manually pick the targets that the software could not recognize due to fisheye distortion. This operation was necessary in order to optimize the calculation of the camera alignment.
Each project was divided into different steps: i) Automatic alignment, ii) adding markers (automatically and manually) and optimization, iii) adding references distance and optimization, iiii) optimization considering also the topographic measurement. The precision obtained from each step was monitored with the purpose of understanding the degree of automatism that can be reached when using fisheye methodology and where the human intervention is needed in the process. The steps involved are listed in the table in Figure 11.

4.4 Final results

4.4.1 Canon 5D MIII - Sigma 8mm equisolid fisheye

The tests carried out with this configuration produced the best results, as the obtained point cloud shows a very precise alignment with the scans obtained via laser scanner (Figure 12).
Two elaborations were obtained from this configuration: the first one, less precise, preceded the methodology that has been here illustrated; and the second one was instead obtained after. It is interesting to point out that in the first test, the precision obtained was much lower than that the one obtained with the second test. The difference between these two processes resides in the different radius used to crop the photos: the first one was hypothesized, whereas the second one was accurately measured (more stringent) from a precise calculation with the previously discussed formulas.

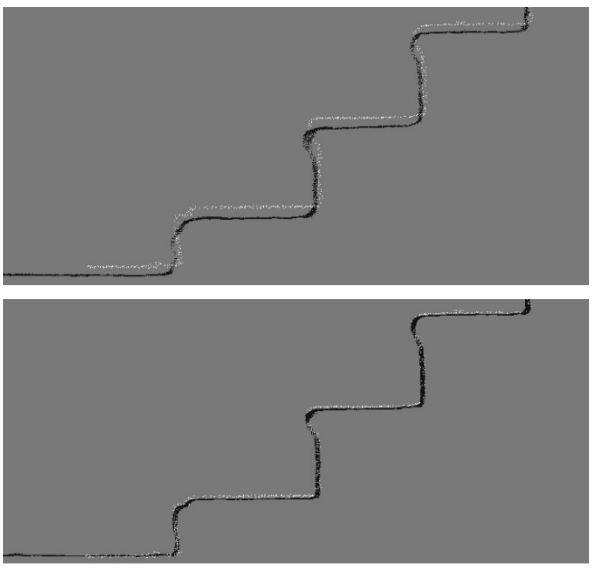

Figure 12. Comparison among the laser scan (white) and photogrammetric point cloud (black). On top the first elaboration using the 5D and the sigma 8mm, in the bottom the second.

4.4.2 Nikon d 810 – Samyang 12mm stereographic fisheye

The alignment obtained with this configuration produces a lower precision than that obtained with the Canon configuration, but still within the limits of the chosen representation scale (Figure 13). Although in theory it seemed to be the best case scenario, the results achieved with the 12mm fisheye lens were just acceptable and not in accordance with either the expectations or the previously performed tests. The reason of this behavior cannot be completely understood, and are probably due to a slight difference in the capturing geometry or in the photo quality.

4.4.3 Nikon D810 - Sigma 12mm rectilinear

The test with the Sigma 12mm rectilinear lens was performed in order to compare the fisheye lens with an ultra wide-angle rectilinear lens. In particular, this lens was chosen because its FOV is very close to those obtained with the fisheyes after the cropping phase. Despite the higher number of photos (945 photos) used and the shooting geometry modified to deal with the field of view of this lens, the results obtained were far below the expectations and far below the results obtained with the fisheye lenses. The cause of this is to be identified in the capturing

geometry: the narrow spaces cannot be surveyed by a rectilinear lens, even a wide-angle lens without shooting a very high number of photos.

Figure 13. Dense point cloud obtained with the Nikon D810 coupled with 12mm stereographic fisheye.

5. CONCLUSIONS

The conducted research led to the design and implementation of a complete photogrammetric survey of complex environments characterized by very narrow spaces, scarce illumination and intricate geometry. The idea is to use fisheye lenses and find rules that can standardize this type of survey and the ensuing elaboration process. The theory of fisheye distortion and some preliminary tests suggest to concentrate the attention on the non-uniform distribution of the image resolution. The idea is to use only the portion of image that provides the maximum acceptable GSD for the desired restitution scale. The first outcome of this approach could be an application that can be used to calculate for each scenario the cropping mask to be applied to fisheye images in order to handle the final accuracy of the model.
In this way, after cropping the images, the FOV will be slightly reduced, but the portions of the images that are not suitable for the chosen representation scale can be discarded. As results, alignment and matching are improved, and the process produces more reliable results and less noisy dense point cloud; it could also help the camera calibration model by removing the most distorted portion of the frame. The best results were obtained using the Sigma 8mm equisolid fisheye and in this case the use of the cropping method was very successful.
The remaining issue is the very complex capturing geometry that has to be arranged case by case. No standards can be followed a priori. Maintaining a 1:1 base distance/capturing distance ratio can guarantee the correct number of images and the suitable overlap. The use of a large number of markers and a lot of manual refining work represented the key of the success in the process: a complete autonomous elaboration when using fisheye lenses can only lead to a failure. Topographic data are necessary to improve the final accuracy.
The presented case of study is particularly challenging considering the complexity of the geometry and the cylindrical shape of the space. For this reasons, it was chosen to stress the presented methodology.
Future work could include the development of a ready-made instrument based on multiple fisheye lenses, able to speed up the acquisition phase and regularize the capturing geometry and thus avoid the small imperfections that cause a decay of the result.

6. ACKNOWLEDGEMENTS

Veneranda Fabbrica of Milan's Cathedral supported this work. Special thanks to the director Eng. Francesco Canali and to all staff especially Francesco Aquilano and Massimiliano Regis.

7. REFERENCES

Fassi, F., Achille, C., Mandelli, A., Rechichi, F., and Parri, S., 2015. A new idea of bim system for visualization, web sharing and using huge complex 3d models for facility management. In: *The International Archives of the Photogrammetry, Remote Sensing and Spatial Information Sciences*, XL-5/W4, 359-366, doi:10.5194/isprsarchives-XL-5-W4-359-2015, 2015.

Covas J., Ferreira V. and Mateus L., 2015. 3D reconstruction with fisheye images strategies to survey complex heritage buildings. In: *2015 Digital Heritage*, Granada, 2015, pp. 123-126. doi: 10.1109/DigitalHeritage.2015.7413850

Kannala J, Brandt SS., 2006. A generic camera model and calibration method for conventional, wide-angle, and fish-eye lenses. In: *IEEE transactions pattern analysis and machine intelligence*, 2006 Aug; 28(8):1335-40.

Marčiš, M., Barták, P., Valaška, D., Fraštia, M., and Trhan, O., (2016). Use of image based modelling for documentation of intricately shaped objects. In: *The International Archives of the Photogrammetry, Remote Sensing and Spatial Information Sciences*, XLI-B5, 327-334, doi:10.5194/isprs-archives-XLI-B5-327-2016.

Nocerino, E., Menna, F., and Remondino, F., 2014. Accuracy of typical photogrammetric networks in cultural heritage 3d modeling projects. In: *The International Archives of the Photogrammetry, Remote Sensing and Spatial Information Sciences*, XL-5, 465-472, doi:10.5194/isprsarchives-XL-5-465-2014.

Pierrot-Deseilligny, M., and Clery, I., 2011. APERO, an open source bundle adjustment software for automatic calibration and orientation of set of images. In: The International Archives of the Photogrammetry, Remote Sensing and Spatial Information Sciences, 5/W16, 2011.

Ray, S. F., 2002. Applied Photographic Optics: Lenses and Optical Systems for Photography, Film, Video and Electronic Imaging. Focal Press.